Higgs-induced flavor-changing neutral current as a source of new physics in $b \to s$ transitions

Anjan S. Joshipura* and Bhavik P. Kodrani†

Physical Research Laboratory, Navarangpura, Ahmedabad 380 009, India

(Received 31 October 2009; published 16 February 2010)

The experimental study of B mesons suggest the existence of some new physics contribution to the $B_s^0 - \bar{B}_s^0$ mixing. We study the implications of a hypothesis that this contribution is generated by the Higgs-induced flavor-changing neutral currents (FCNC). We concentrate on the specific $b \to s$ transition which is described by two complex FCNC parameters, F_{23} and F_{32}, and parameters in the Higgs sector. Model-independent constraints on these parameters are derived from the $B_s^0 - \bar{B}_s^0$ mixing and are used to predict the branching ratios for $\bar{B}_s \to \mu^+\mu^-$ and $\bar{B}_d \to \bar{K}\mu^+\mu^-$ numerically by considering general variations in the Higgs parameters assuming that Higgs sector conserves CP. Taking the results on $B_s^0 - \bar{B}_s^0$ mixing derived by the global analysis of UTfit group as a guide we present the general constraints on $F_{23}^* F_{32}$ in terms of the pseudoscalar mass M_A. The former is required to be in the range $\sim$(1–5) $\times 10^{-11} M_A^2$ GeV^{-2} if the Higgs-induced FCNC represent the dominant source of new physics. The phases of these couplings can account for the large CP violating phase in the $B_s^0 - \bar{B}_s^0$ mixing except when $F_{23} = F_{32}$. The Higgs contribution to $\bar{B}_s \to \mu^+\mu^-$ branching ratio can be large, close to the present limit while it remains close to the standard model value in case of the process $\bar{B}_d \to \bar{K}\mu^+\mu^-$ for all the models under study. We identify and discuss various specific examples which can naturally lead to suppressed FCNC in the $K^0 - \bar{K}^0$ mixing allowing at the same time the required values for F_{23}^* and F_{32}.

DOI: 10.1103/PhysRevD.81.035013 PACS numbers: 12.60.Fr, 11.30.Er, 12.15.Mm

I. INTRODUCTION

The Cabibbo Kobayashi Maskawa (CKM) matrix V provides a unique source of flavor and CP violations in the standard model (SM). It leads to flavor-changing neutral currents (FCNC) at the one loop level. K and B meson decays and mixing have provided stringent tests of these FCNC induced processes and the SM predictions have been verified with some hints for possible new physics contributions [1–3]. Any new source of flavor violations resulting from the well-motivated extensions of the SM (e.g. supersymmetry) is now constrained to be small [4,5].

Uncovering highly constrained new physics becomes easier if one specifically looks at observables which are predicted to be small or zero in the SM. Transitions between the b and s quarks offer such observables [6]. The $b \leftrightarrow s$ transitions among other things lead to (1) $\Delta B = 2$, $B_s^0 - \bar{B}_s^0$ mixing, (2) the leptonic decays $\bar{B}_s \to l^+l^-(l = e, \mu, \tau)$, (3) the semileptonic decays $\bar{B}_d \to (\bar{K}, \bar{K}^*)\mu^+\mu^-$. The CP violating phase

$$\phi_s = \mathrm{Arg}\left(-\frac{M_{12}}{\Gamma_{12}}\right)$$

is predicted to be quite small $\sim 0.2°$ in the SM. Here M_{12} and Γ_{12} denote the real and absorptive parts of $B_s^0 - \bar{B}_s^0$ transition amplitude, respectively. In contrast, the experimental determination of ϕ_s from the time-dependent CP asymmetry in $B_s \to J/\psi\phi$ decays by the D0 [7] and CDF [8] groups allow much larger phase: the 90% C.L. average reported by HFAG [9] requires $[-1.47; -0.29] \cup [-2.85; -1.65]$. By including the D0 and the CDF results in their global analysis, UTfit group find around 3σ departure from the SM prediction on ϕ_s [4,10]. Similar analysis by the CKMfitter group [5] also reports deviation from the SM result but at around 2.5σ. This may be a hint of the presence of new physics in the $b \leftrightarrow s$ transitions. Future measurement would provide a crucial test of this possibility.

The decay rate for $\bar{B}_s \to \mu^+\mu^-$ is also predicted [11] to be small in SM,

$$\mathrm{Br}(\bar{B}_s \to \mu^+\mu^-) = (3.51 \pm 0.50) \times 10^{-9}, \tag{1}$$

compared to an order of magnitude larger experimental limit [12]

$$\mathrm{Br}(\bar{B}_s \to \mu^+\mu^-) < 5.8 \times 10^{-8} (95\%\ \mathrm{C.L.}). \tag{2}$$

This rate therefore can be an important observable in search of new physics. In contrast, the branching ratios for the exclusive processes in (3) are close to the SM predictions. But they still provide valuable constraints on any new physics that may be present. Moreover, the dilepton spectrum and the angular distribution of leptons in these exclusive processes provide very sensitive test of the SM and possible indication of new physics [13,14]. The LHCb [15] and the super-B factory will allow more sensitive determination of these observables and will strongly constrain or uncover any new physics that may be present.

The $b \leftrightarrow s$ transition is also interesting from the theoretical point of view since several extensions of SM predict

*anjan@prl.res.in
†bhavik@prl.res.in

relatively large effects in this transition. The most popular extensions studied are the two Higgs doublet models (2HDM) in which some symmetry (discrete or super) prevents FCNC at the tree level. In these models, the Higgs (like the W boson) contribute to the FCNC at the loop level. The supersymmetric standard model is one such example within which the Higgs and sparticle mediated flavor-changing effects have been extensively studied [16]. In the minimal supersymmetric standard model (MSSM), the $d_i \leftrightarrow d_j$ transitions between the charged $-1/3$ quarks in large tanβ limit are governed by the CKM factor $V_{3i}V_{3j}^*$ [17–19]. As a result, the effect becomes more prominent for the $b \leftrightarrow s$ transitions compared to others. The same thing also happens in the charged Higgs-induced flavor transitions in certain class of two Higgs doublet models. Quarks and leptons would couple and obtain their masses from both the Higgs doublets in a general 2HDM. This however leads to the Higgs-induced FCNC at the tree level. This is generally avoided [20] by imposing a discrete symmetry which ensures that all the fermions of a given charge obtain their masses from coupling to only one Higgs [21] doublet. This way of suppressing FCNC is technically natural since the loop induced FCNC couplings after spontaneous breaking of the discrete symmetry are calculable and finite. This way of suppressing FCNC is termed as natural flavor conservation (NFC) in the literature [20]. The charged Higgs-induced $d_i \leftrightarrow d_j$ transitions in these models also involve the factor $V_{3i}V_{3j}^*$ as in the MSSM.

2HDM with NFC and the MSSM realize the minimal flavor violation (MFV) [22] scenario and do not have any additional CP violating phase other than the CKM phase. In the context of the MSSM, one can consider scenarios which go beyond the MFV to accommodate a large ϕ_s [16,23]. This cannot easily be done for a two Higgs doublet model with NFC. Large CP violating phases are possible in more general two Higgs doublet models (called type-III 2HDM) which allow the tree level FCNC. Most general model of this type can lead to large flavor violation in the $d \leftrightarrow s$ transitions and would imply a very heavy Higgs mass suppressing all other flavor violations. It is possible to imagine scenarios where the tree level FCNC couplings also show hierarchy as in the quark masses [24]. This class of models would imply relatively large flavor violations in B transitions. The standard example of this is the so called Cheng-Sher ansatz [25] which postulates a relation between the down quark masses m_i and the FCNC couplings:

$$F_{ij} = \lambda_{ij}\frac{\sqrt{m_i m_j}}{v}, \tag{3}$$

with $\lambda_{ij} \sim \mathcal{O}(1)$ and $v \sim O(174\ \text{GeV})$.

There exist explicit models [26–28] which lead to hierarchy in FCNC. Such models which are theoretically as natural as the two Higgs doublets with NFC can lead to interesting patterns of flavor violations. Our aim in this paper is to analyze the constrains and prediction of the Higgs-induced tree level FCNC in the $b \leftrightarrow s$ transitions. Rather than looking at any specific model in this category we consider several classes of models which imply interesting patterns of flavor violation. We find that the predictions of some of these models for the leptonic and semileptonic transitions mentioned above are distinctively different compared to the two Higgs doublet models with NFC and the MSSM. Moreover, it is possible within them to simultaneously look at the constraints from all three processes listed above and we find that the $B_s^0 - \bar{B}_s^0$ mixing provides very stringent restrictions on the other two processes.

There have been earlier phenomenological studies of models with tree level FCNC [29]. Most of these are model specific and mainly use the Cheng-Sher ansatz and try to constrain parameters λ_{ij}. As we discuss, there are models which are distinctively different from this ansatz. So rather than specifying any specific model, we perform a model-independent analysis of the Higgs-induced FCNC couplings. Unlike the Cheng-Sher ansatz, these couplings in general can have phases which are not included in the earlier analysis. As we show, the FCNC couplings may provide the source of a large ϕ_s and we identify models which explain large ϕ_s and those which cannot do so.

We present the general structure of the Higgs-induced FCNC in the next section where we also discuss various classes of models which lead to hierarchical FCNC couplings. In Sec. III, we give the details of the effective Hamiltonian for the $\Delta B = 1$ and 2 transitions. In the next section, we derive an important relation between the Higgs contributions to the $B_s^0 - \bar{B}_s^0$ mass difference and to the branching ratio for $\bar{B}_s \to \mu^+\mu^-$. This relation is independent of the FCNC couplings F_{23}^*, F_{32} under specific assumptions. In the same section, we study numerical implications of various classes of models and conclude in the last section.

II. FCNC: STRUCTURE AND EXAMPLES

This section is devoted to a discussion of classes of the 2HDM which we use as a guide to carry out a fairly model-independent analysis of the $b \to s$ transitions subsequently.

The general two Higgs doublet models [20] have the following Yukawa couplings in the down quark sector:

$$-\mathcal{L}_Y^d = \bar{d}_L'(\Gamma_1\phi_1^0 + \Gamma_2\phi_2^0)d_R' + \text{H.c.}. \tag{4}$$

Here, $d_{L,R}'$ denote (the column of) the weak eigenstates of down quarks. The models with NFC impose an additional discrete symmetry, e.g. $(d_R', \phi_1) \to -(d_R', \phi_1)$ which forbids the couplings Γ_2. As a result, the down quark couplings to ϕ_1 become diagonal in the mass basis and there are no tree level FCNC.

More general 2HDM allow both Γ_1 and Γ_2 in Eq. (4) and contain the tree level FCNC. Consider two orthogonal combinations of the Higgs fields ϕ_1, ϕ_2:

$$\phi^0 \equiv \cos\beta\phi_1^0 + \sin\beta\phi_2^0, \tag{5}$$

$$\phi_F^0 \equiv -\sin\beta\phi_1^0 + \cos\beta\phi_2^0, \tag{6}$$

with $\langle\phi\rangle_1 = v\cos\beta$, $\langle\phi\rangle_2 = v\sin\beta$, and $v \sim 174$ GeV. ϕ^0 acquires a nonzero vacuum expectation value (vev) and leads to the quark mass matrix

$$M_d = v(\Gamma_1\cos\beta + \Gamma_2\sin\beta). \tag{7}$$

ϕ is like the SM Higgs field with flavor conserving couplings to quarks. The ϕ_F violates flavor and one can write using, Eqs. (4) and (7)

$$-\mathcal{L}_{\rm FCNC} = \sum_{i=j} F_{ij}\bar{d}_{iL}d_{jR}\phi_F^0 + \text{H.c.}. \tag{8}$$

$d_{L,R}$ denote the mass eigenstates,

$$F_{ij} \equiv (V_L^\dagger\Gamma_2 V_R)_{ij}\frac{1}{\cos\beta} \tag{9}$$

and $V_{L,R}$ are defined by

$$V_L^\dagger M_d V_R = D_d. \tag{10}$$

Here D_d is the diagonal mass matrix for the down quarks. The structure as in (8) can arise as an effective interactions from the loop diagrams as in MSSM [17] or the 2HDM with NFC [30]. Phenomenology based on this structure therefore would include such cases also.

The leptonic and semileptonic FCNC transitions also depend on how the charged leptons couple to the fields $\phi_{1,2}$. For definiteness, we will assume that the charged lepton Yukawa couplings are given as in the MSSM. We thus assume

$$-\mathcal{L}_Y^l = \bar{l}'_L\Gamma_1^l l'_R\phi_1^0 + \text{H.c.}, = \frac{1}{v\cos\beta}\bar{l}_L D_l l_R\phi_1^0 + \text{H.c.}. \tag{11}$$

If coupling to ϕ_2 is also present then one would get flavor violations in the leptonic sector also.

General properties of F follow from its definition, Eq. (9). We shall consider three specific class of FCNC and show that each of these imply different and interesting physics.

(A) Hermitian structures: Assume that quark mass matrices and $\Gamma_{1,2}$ are Hermitian. In this case, Eq. (9) trivially implies

$$F_{ij} = F_{ji}^*. \tag{12}$$

(B) Symmetric structures: Assume that M_d and $\Gamma_{1,2}$ are symmetric. This trivially leads to symmetric FCNC couplings:

$$F_{ij} = F_{ji}. \tag{13}$$

(C) MSSM like structures: The FCNC in MSSM in large $\tan\beta$ limit [17,19] can be described by an effective tree level Lagrangian similar to Eq. (9) with the specific relation

$$F_{ij} = \frac{m_j}{m_i}F_{ji}^* \tag{14}$$

between the FCNC couplings. The same relation also holds in general 2HDM with NFC where F_{ij} are induced by the charged Higgs at 1-loop [30]. More interestingly, even the tree level FCNC can satisfy the same relation in some specific models [26,27].

While the phenomenological analysis that we present in the above three cases would be model-independent, we give below several examples of textures/models which can realize above scenarios and simultaneously explain the quark masses.

Yukawa textures and FCNC

The strongest constraints on FCNC come from the $K^0-\bar{K}^0$ mixing and the ϵ parameter. One needs very heavy Higgs ~O(TeV) to suppress this effect if $F_{12} \sim$ O (gauge coupling). Heavy Higgs would then suppress other flavor violations as well without leaving any signature at low energy. Interesting class of models would be the ones in which the coupling $|F_{12}|$ would be suppressed compared to the other couplings. As already discussed in the introduction, widely studied example of this is the Cheng-Sher ansatz, Eq. (3). Here the suppression in F_{ij} comes from the suppression in the quark masses compared to the weak scale. F_{ij} may also be suppressed by mixing angles. This can come about naturally in large classes of 2HDM. Assume that the Higgs ϕ_2 in Eq. (4) is responsible for only the third generation mass while the Higgs ϕ_1 accounts for the first two generation masses and the intergeneration mixing. Only the (33) element of Γ_2 is assumed nonzero in this case and Eq. (9) automatically implies

$$F_{ij} = \frac{m_b}{v\cos\beta\sin\beta}V_{L3i}^*V_{R3j}. \tag{15}$$

If M_d is Hermitian or symmetric one automatically obtains Eqs. (12) and (13). If the off-diagonal elements of $V_{L,R}$ are suppressed compared to the diagonal elements, then F_{12} will be more suppressed compared to others. In particular, $(V_{L,R})_{3i} \sim c_{L,R}\sqrt{\frac{m_i}{m_b}}$ reproduces the Cheng-Sher ansatz with $\lambda_{ij} \sim \frac{c_L c_R}{\cos\beta\sin\beta}$. Thus this class of models may be regarded as a generalization of the Cheng-Sher ansatz.

Let us take two concrete examples which are among the specific textures studied in the literature with a view to understand the fermion masses and mixings.

Consider

(i)

$$\Gamma_1 = y_{33}\begin{pmatrix} d\epsilon^4 & b\epsilon^3 & c\epsilon^3 \\ b\epsilon^3 & f\epsilon^2 & a\epsilon^2 \\ c\epsilon^3 & a\epsilon^2 & 0 \end{pmatrix}; \qquad \Gamma_2 = y_{33}\begin{pmatrix} 0 & 0 & 0 \\ 0 & 0 & 0 \\ 0 & 0 & 1 \end{pmatrix}. \tag{16}$$

These couplings together imply the down quark mass matrix studied long ago by Roberts, Romanino, Ross, and Velesco-Sevilla [31] and recently in [32]. ϵ here is a small parameter which can be determined from the quark masses. $\epsilon \sim 0.1$ is determined in [32] assuming the above structure to be valid at the grand unified theory (GUT) scale. Above matrices imply in a straightforward way

$$\begin{aligned} |V_{L32}| &= |V^*_{R32}| \sim a\epsilon^2; \\ |V_{L31}| &= |V^*_{R31}| \sim |c|\epsilon^3; \\ |V_{L12}| &= |V^*_{R12}| \sim \frac{b}{f}\epsilon. \end{aligned} \tag{17}$$

This in turn implies

$$\begin{aligned} |F_{12}| &\approx \frac{m_b}{v\cos\beta\sin\beta} a|c|\epsilon^5; \\ |F_{13}| &\approx \frac{m_b}{v\cos\beta\sin\beta}|c|\epsilon^3; \\ |F_{23}| &\approx \frac{m_b}{v\cos\beta\sin\beta} a\epsilon^2. \end{aligned} \tag{18}$$

Thus one obtains the desired hierarchical FCNC couplings with this ansatz.

(ii) As an other example we consider the texture suggested in [33]:

$$\Gamma_1 = y_{33}\begin{pmatrix} d\epsilon^6 & b\epsilon^4 & c\epsilon^3 \\ b\epsilon^4 & f\epsilon^2 & a\epsilon \\ c\epsilon^3 & a\epsilon & 0 \end{pmatrix}; \qquad \Gamma_2 = y_{33}\begin{pmatrix} 0 & 0 & 0 \\ 0 & 0 & 0 \\ 0 & 0 & 1 \end{pmatrix}, \tag{19}$$

where ϵ is a small expansion parameter (assumed to be $\sim$0.2 in [33]) and other parameters are O(1). The quark mass matrix is of rank 1 if these parameters are exactly 1. Because of this feature, it is possible to simultaneously understand the large mixing in the neutrinos and small mixing in the quark sector. The above form of the quark matrix also implies the relation

$$(V_L)_{ij} \approx (V_L)_{ji} \approx \sqrt{\frac{m_i}{m_j}}, \qquad (i < j).$$

As a result, the FCNC couplings satisfy the Cheng-Sher ansatz given in Eq. (3) with $\lambda_{ij} \sim \frac{1}{\cos\beta\sin\beta}$. M_d and Yukawa couplings are symmetric in both the above examples. One could consider instead similar Hermitian textures as well.

(iii) Somewhat different illustration of the suppressed FCNC couplings is provided by the following textures of the Yukawa couplings:

$$\Gamma_1 = \begin{pmatrix} x & x & x \\ x & x & x \\ 0 & 0 & 0 \end{pmatrix}; \qquad \Gamma_2 = \begin{pmatrix} 0 & 0 & 0 \\ 0 & 0 & 0 \\ x & x & x \end{pmatrix}, \tag{20}$$

where x denotes an entry which is not required to be zero. It is straightforward to show that the above Yukawa couplings imply

$$F_{ij} = \frac{1}{v\cos\beta\sin\beta} V^*_{L3i} V_{L3j} m_j \tag{21}$$

and therefore satisfy relation (14). Note that F_{ij} depend only on the left-handed mixing matrix and they remain suppressed and hierarchical if the mixing elements show hierarchy. The structure of FCNC in this example is different compared to the Cheng-Sher ansatz and earlier two examples. The earlier two examples reduce to the Cheng-Sher ansatz if $V_{Lij} \approx V_{Lji} \approx \sqrt{\frac{m_i}{m_j}}$, $(i < j)$ while Eq. (21) has an additional suppression by $\frac{m_j}{m_b}$ compared to them in this case when $j \neq 3$.

This particular example of the suppressed FCNC couplings was proposed in [26]. The hierarchy among F_{ij} is determined in the MSSM by the CKM matrix elements while here it is determined by the elements of the down quark mixing matrix. In particular, the F_{ij} can have new phases not present in the MSSM case. It is possible to construct models [27] in which V_L in Eq. (21) gets replaced by the CKM matrix making the F_{ij} very similar to the MSSM model. Phenomenological consequences of this were studied in [34].

The examples given here are representative rather than exhaustive. One could consider several similar structures, e.g. one based on the Fritzsch ansatz [35] or on some different textures, e.g. based on the μ-τ interchange symmetry [36] all with the property of the suppressed and hierarchical FCNC. Without subscribing to any specific model we shall now consider the general implications for the $b \leftrightarrow s$ transitions.

III. EFFECTIVE HAMILTONIAN FOR THE $b \leftrightarrow s$ TRANSITIONS

The basic interaction in Eq. (8) leads to both $\Delta B = 1$ and 2 transitions. We give below the corresponding effective Hamiltonian.

A. $B_s^0 - \bar{B}_s^0$ mixing

$B_s^0 - \bar{B}_s^0$ mixing is governed by the transition amplitude [37]

$$M_{12}^{*s} \equiv \langle \bar{B}_s^0 | \mathcal{H}_{\rm eff} | B_s^0 \rangle.$$

Here,

$$\mathcal{H}_{\rm eff} \equiv \mathcal{H}_{\rm eff}^{\rm SM} + \mathcal{H}_{\rm eff}^{\rm NP}$$

includes the SM and the new physics contribution to the $B_s^0 - \bar{B}_s^0$ transition. $\mathcal{H}_{\rm eff}^{\rm NP}$ arises in the present case from the tree level exchange of the ϕ_F^0 field and its complex conjugate. We use the parametrization and treatment given in [19] to evaluate the effective Hamiltonian.

$$\mathcal{H}_{\rm eff}^{\rm NP} = \frac{G_F^2 M_W^2}{16\pi^2}(V_{tb}^* V_{ts})[Q_2^{LR} C_2^{LR} + Q_1^{LL} C_1^{LL} + Q_1^{RR} C_1^{RR}]. \tag{22}$$

Here, G_F is the Fermi coupling constant, M_W is the mass of the W boson and V denotes the CKM matrix. The operators Q induced by the FCNC couplings in this case are defined by

$$Q_2^{LR} = (\bar{b}_L s_R)(\bar{b}_R s_L); \qquad Q_1^{LL} = (\bar{b}_R s_L)(\bar{b}_R s_L); \qquad Q_1^{RR} = (\bar{b}_L s_R)(\bar{b}_L s_R).$$

The coefficients $C_{1,2}$ are the Wilson coefficients of these operators evaluated at the Higgs mass scale. They follow from the tree level Feynman diagrams involving the neutral Higgs field ϕ_F^0 and can be evaluated in a straightforward manner:

$$\begin{aligned} C_2^{LR} &= -\frac{16\pi^2}{G_F^2 M_W^2 (V_{tb}^* V_{ts})^2} F_{32} F_{23}^* \langle \phi_F | \phi_F^* \rangle, \\ C_1^{LL} &= -\frac{1}{2}\frac{16\pi^2}{G_F^2 M_W^2 (V_{tb}^* V_{ts})^2} F_{23}^{*2} \langle \phi_F^* | \phi_F^* \rangle, \\ C_1^{RR} &= -\frac{1}{2}\frac{16\pi^2}{G_F^2 M_W^2 (V_{tb}^* V_{ts})^2} F_{32}^{2} \langle \phi_F | \phi_F \rangle. \end{aligned} \tag{23}$$

Here $\langle \phi_F | \phi_F \rangle$ is i times the propagator of ϕ_F^0 field evaluated at the zero momentum transfer and $\langle \phi_F | \phi_F^* \rangle$ and $\langle \phi_F^* | \phi_F^* \rangle$ are defined analogously. These propagators are evaluated by decomposing the ϕ_F^0 field in terms of the Higgs mass eigenstates denoted as h, H (scalars) and A (pseudoscalar). We shall assume that CP is conserved in the Higgs sector in which case decomposition of ϕ_F^0 is given by

$$\begin{aligned} {\rm Re}\,(\phi_F^0) &= \frac{1}{\sqrt{2}}(\cos(\alpha - \beta) h + \sin(\alpha - \beta) H), \\ {\rm Im}(\phi_F^0) &= \frac{1}{\sqrt{2}} A, \end{aligned} \tag{24}$$

where $M_{h,H,A}$ are the masses of the fields h, H, A, respectively. Using these expressions, one arrives at

$$\begin{aligned} \langle \phi_F | \phi_F^* \rangle &= \frac{\sin^2(\alpha - \beta)}{2M_H^2} + \frac{\cos^2(\alpha - \beta)}{2M_h^2} + \frac{1}{2M_A^2}, \\ \langle \phi_F | \phi_F \rangle &= \langle \phi_F^* | \phi_F^* \rangle \\ &= \frac{\sin^2(\alpha - \beta)}{2M_H^2} + \frac{\cos^2(\alpha - \beta)}{2M_h^2} - \frac{1}{2M_A^2}. \end{aligned} \tag{25}$$

Taking the matrix elements of Eq. (22) between the $\bar{B}_s^0$ and B_s^0 mesons one arrives at [19]

$$(M_{12}^{s*})^{\rm NP} = \frac{G_F^2 M_W^2}{48\pi^2} M_{B_s} f_{B_s}^2 (V_{tb}^* V_{ts})^2 [P_2 C_2^{LR} + P_1 C_1^{LL} + P_1 C_1^{RR}], \tag{26}$$

and M_{B_s}, f_{B_s} are the mass and the decay constant of the B_s meson. $P_{1,2}$ summarize the effect of the evolution to the low scale and of the bag factors. When Higgs scale is identified with the top mass one gets, $P_2 \approx 2.56$ and $P_1 \approx -1.06$ [19]. For definiteness, we will use these values in the numerical analysis. The total mixing amplitude is given by

$$\begin{aligned} M_{12}^{s*} &= (M_{12}^{s*})^{\rm SM} + (M_{12}^{s*})^{\rm NP} \\ &\equiv (M_{12}^{s*})^{\rm SM}(1 + \kappa_s^H e^{2i(\phi_s^H + \beta_s)}). \end{aligned} \tag{27}$$

The $(M_{12}^{*s})^{\rm SM}$ is given [37] by

$$(M_{12}^{*s})^{\rm SM} = \frac{G_F^2 M_W^2 M_{B_s} f_{B_s}^2 B_{B_s} \eta_B}{12\pi^2} (V_{tb}^* V_{ts})^2 S_0(x_t), \tag{28}$$

with $S_0(x_t) \approx 2.3$ for $m_t \approx 161$ GeV and $\eta_B \approx 0.55$ represents the QCD corrections. Using Eq. (23) we find

$$\begin{aligned} \kappa_s^H e^{2i\phi_s^H} = &-\frac{4\pi^2}{B_{B_s} \eta_B S_0(x_t) G_F^2 M_W^2 |V_{tb}^* V_{ts}|^2} \\ &\times \Big[P_2 F_{32} F_{23}^* \langle \phi_F | \phi_F^* \rangle \\ &+ \frac{1}{2} P_1 (F_{32}^2 \langle \phi_F | \phi_F \rangle + F_{23}^{*2} \langle \phi_F | \phi_F \rangle^*) \Big]. \end{aligned} \tag{29}$$

The new physics induced phase in the above expression is determined by the phases of the FCNC couplings and the complex Higgs propagators. We assume throughout that the Higgs sector is CP conserving. In this case, the only source of the nonstandard CP violation resides in the phases of F_{23}, F_{32}.

B. $\Delta B = 1$ transitions

The transition $b \to s$ occurs in SM at the 1-loop level. The corresponding effective Hamiltonian is described in terms of 10 different operators and associated Wilson coefficients. The complete list can be found, for example, in [13]. The Wilson coefficients are calculated at the electroweak scale and are then evaluated in the low energy theory in a standard way. If some new physics is present at or above the electroweak scale then (1) it can give additional contributions to some of the Wilson coefficients and/

or (2) can lead to new sets of operators not present in the SM. We will mainly be concerned here with effects due to (2) induced by the presence of the nonstandard Higgs field (s) but the effect (1) may also be simultaneously present.

The Higgs-induced operators for the transition $b \to s\mu^+\mu^-$ may be parametrized as

$$\mathcal{H}^H_{\rm eff} \equiv -\frac{4G_F}{\sqrt{2}} V_{tb}V_{ts}^* \sum_{i=S,S',P,P'} C_i(\mu)O_i(\mu), \tag{30}$$

where μ denotes the renormalization scale at which the operators and the Wilson coefficients appearing above are defined. The operators are defined as

$$O_S = \frac{e^2}{16\pi^2}\bar{s}_L b_R \bar{\mu}\mu; \qquad O_P = \frac{e^2}{16\pi^2}\bar{s}_L b_R \bar{\mu}\gamma_5\mu;$$
$$O'_S = \frac{e^2}{16\pi^2}\bar{s}_R b_L \bar{\mu}\mu; \qquad O'_P = \frac{e^2}{16\pi^2}\bar{s}_R b_L \bar{\mu}\gamma_5\mu. \tag{31}$$

The tree level Higgs exchange through Eq. (8) induce the above operators with the Wilson coefficients given by

$$C_S = -\frac{\sqrt{2}\pi}{\alpha G_F V_{tb}V_{ts}^*}\frac{F_{23}m_\mu}{2v\cos\beta}\left(\frac{\sin(\alpha-\beta)\cos\alpha}{M_H^2} - \frac{\cos(\alpha-\beta)\sin\alpha}{M_h^2}\right),$$
$$C'_S = -\frac{\sqrt{2}\pi}{\alpha G_F V_{tb}V_{ts}^*}\frac{F^*_{32}m_\mu}{2v\cos\beta}\left(\frac{\sin(\alpha-\beta)\cos\alpha}{M_H^2} - \frac{\cos(\alpha-\beta)\sin\alpha}{M_h^2}\right),$$
$$C_P = -\frac{\sqrt{2}\pi}{\alpha G_F V_{tb}V_{ts}^*}\frac{F_{23}m_\mu}{2v\cos\beta}\frac{\sin\beta}{M_A^2},$$
$$C'_P = -\frac{\sqrt{2}\pi}{\alpha G_F V_{tb}V_{ts}^*}\frac{F^*_{32}m_\mu}{2v\cos\beta}\left(-\frac{\sin\beta}{M_A^2}\right). \tag{32}$$

Equation (30) contributes both to the $\bar{B}_s \to \mu^+\mu^-$ and the $\bar{B}_d \to \bar{K}(\bar{K}^*)\mu^+\mu^-$ processes. The Higgs contribution to the branching ratio for the former process follows [13,30] in a straightforward way from Eq. (30):

$$\mathrm{Br}(\bar{B}_s \to \mu^+\mu^-) = \left(\frac{\alpha G_F|V_{tb}V_{ts}^*|}{\sqrt{2}\pi}\right)^2 \frac{f_{B_s}^2 M_{B_s}^5 \tau_{B_s}}{32\pi(m_b+m_s)^2} \times\left(1-\frac{4m_\mu^2}{M_{B_s}^2}\right)^{1/2}\left(\left(1-\frac{4m_\mu^2}{M_{B_s}^2}\right)|C_S - C'_S|^2 + \left|C_P - C'_P + 2\frac{m_\mu}{M_{B_s}^2}C_{10}\right|^2\right). \tag{33}$$

The explicit expression for C_{10} in SM can be found, for example, in [38]. In view of the smallness of this contribution, we would be interested in exploring the region of parameter space where the Higgs contribution significantly dominates over the contribution from C_{10}. It is thus useful to separate out the Higgs contribution B_H alone to the above branching ratio and we define

$$B_H \equiv \left(\frac{\alpha G_F|V_{tb}V_{ts}^*|}{\sqrt{2}\pi}\right)^2 \frac{f_{B_s}^2 M_{B_s}^5 \tau_{B_s}}{32\pi(m_b+m_s)^2}\left(1-\frac{4m_\mu^2}{M_{B_s}^2}\right)^{1/2} \times\left(\left(1-\frac{4m_\mu^2}{M_{B_s}^2}\right)|C_S - C'_S|^2 + |C_P - C'_P|^2\right). \tag{34}$$

We however use the full equation, (33), in our numerical study.

The process $\bar{B}_d \to \bar{K}\mu^+\mu^-$ is studied in detail in [13,14] using the QCD factorization approach which works for the low q^2 region. The amplitude for this process depends on two hadronic form factors defined as [39]

$$\langle K|\bar{s}\gamma_\mu b|\bar{B}\rangle = (2p_B - q)_\mu f_+(q^2) + \frac{M_B^2 - M_K^2}{q^2}q_\mu[f_0(q^2) - f_+(q^2)],$$

where p_B and q, respectively, refer to four momenta of $\bar{B}$ meson and the dilepton pair. Bobeth *et al.* [14] evaluated the form factors using the QCD factorization and results based on the light cone sum rules to obtain predictions (details can be found in the Appendixes A, B of the Ref. [14]) for the angular distribution of the dilepton pair and the branching ratio for $\bar{B}_d \to \bar{K}\mu^+\mu^-$. Restricting the dilepton invariant (mass)^2 between the range 1 GeV$^2 < q^2 < 7$ GeV^2, they derive [14]

$$\mathrm{Br}(\bar{B}_d \to \bar{K}\mu^+\mu^-) = \left(\frac{\tau_B^+}{1.64\ \mathrm{ps}}\right)\left(1.91 + 0.02(|\tilde{C}_S|^2 + |\tilde{C}_P|^2) - \frac{m_\mu}{\mathrm{GeV}}\frac{\mathrm{Re}(\tilde{C}_P)}{2.92} - \frac{m_\mu^2}{\mathrm{GeV}^2}\left(\frac{|\tilde{C}_S|^2}{5.98^2} + \frac{|\tilde{C}_P|^2}{10.36^2}\right) + O(m_\mu^3)\right)\times 10^{-7}, \tag{35}$$

where $\tilde{C}_S$, $\tilde{C}_P$ are given in terms of $C_{S,P}$, $C'_{S,P}$ in Eq. (32) by

$$\tilde{C}_S = C_S + C'_S, \qquad \tilde{C}_P = C_P + C'_P. \tag{36}$$

IV. CONSTRAINING THE FCNC COUPLINGS

Among the processes mentioned above, the $B_s^0 - \bar{B}_s^0$ transition is the most accurately measured and provide sensitive test of the FCNC couplings. In particular, the presence of these couplings in some cases can explain the additional CP violating phase in the $B_s \to J/\psi\phi$ decay.

The new physics contribution to $B_s^0 - \bar{B}_s^0$ mixing is parametrized in terms of

$$C_{B_s} = |1 + \kappa_s^H e^{2i(\phi_s^H + \beta_s)}|,$$
$$\phi_{B_s} = -\frac{1}{2}\,\mathrm{Arg}(1 + \kappa_s^H e^{2i(\phi_s^H+\beta_s)}), \tag{37}$$

where κ_s^H is given in our case by Eq. (29). The 95% allowed ranges of C_{B_s} and ϕ_{B_s} given by UTfit collaboration are [10]

$$C_{B_s} = [0.68, 1.51],$$
$$\phi_{B_s} = [-30.5, -9.9] \cup [-77.8, -58.2]. \tag{38}$$

We shall derive constraints on F_{23}, F_{32} based on the above values and look at its observable consequences for the processes $\bar{B}_s \to \mu^+\mu^-$, $\bar{B}_d \to \bar{K}\mu^+\mu^-$. The derived constraints depend on the Higgs masses and mixing angles. But a simple and F_{ij}-independent correlations between κ_s^H and the Higgs contribution B_H to the branching ratio for the process $\bar{B}_s \to \mu^+\mu^-$ follows in the decoupling limit if it is assumed that the Higgs potential is the same as in the case of MSSM. We first derive this relation. Then we give up these simplifying assumptions in the Higgs sector and explore the Higgs parameter space numerically and study the correlation between κ_s^H and the $\bar{B}_s \to \mu^+\mu^-$ branching ratio.

The Higgs masses and mixing angle satisfy the following two relations [17,20] if the scalar potential coincide with the MSSM:

$$\langle\phi_F|\phi_F\rangle = 0; \qquad \cos^2(\alpha - \beta) = \frac{M_h^2(M_Z^2 - M_h^2)}{M_A^2(M_H^2 - M_h^2)}. \tag{39}$$

The first relation leads to the following simple expression for κ_s:

$$\kappa_s^H e^{2i\phi_s^H} = -\frac{4\pi^2 P_2 F_{32} F_{23}^*}{B_{B_s}\eta_B S_0(x_t) G_F^2 M_W^2 |V_{tb}^* V_{ts}|^2 M_A^2}. \tag{40}$$

Note that

$$e^{2i\phi_s^H} = -\frac{F_{32}F_{23}^*}{|F_{32}F_{23}^*|}$$

directly probes the CP violating phase in the FCNC couplings and would depend on the model for quark masses under consideration.

(i) In models with Hermitian mass matrices, $\phi_s^H = Arg(F_{32}) \pm \pi$. This class of models can account for possible large CP violating phase ϕ_s.

(ii) In contrast, the models with symmetric mass matrices, automatically imply $\phi_s^H = \pm\pi$. Thus even the presence of FCNC in these models does not lead to large CP violation. Alternative source of CP violation can arise in these models if the Higgs sector violate CP. In this case, mixing between the scalar and pseudoscalar generate additional phase which can contribute to ϕ_s^H. This scenario was studied in [34] in a specific model with symmetric quark mass matrices.

(iii) ϕ_s^H is again given by the phase of F_{32} in class (C) models satisfying $F_{32} = \frac{m_s}{m_b}F_{23}^*$. In particular, MSSM with MFV as well as the 2HDM of Ref. [27] predict $F_{32} \sim V_{tb}^* V_{ts}$. As a consequence, the Higgs generated phase ϕ_s^H coincide with the SM phase β_s which is known to be small. Thus, these type of models will also need additional source, e.g. scalar-pseudoscalar mixing if large ϕ_s is established.

The magnitude κ_s^H of the Higgs contribution to the $B_s^0 - \bar{B}_s^0$ mass difference relative to the SM contribution can be quite large for reasonable values of the unknown parameters. Equation (40) implies that

$$\kappa_s^H \approx 0.6\left(\frac{F_{23}^* F_{32}}{10^{-6}}\right)\left(\frac{300\ \mathrm{GeV}}{M_A}\right)^2. \tag{41}$$

Consider various model expectations:

(i) If one uses the Cheng-Sher ansatz Eq. (3) then $|F_{23}F_{32}| \approx \mathcal{O}(1)\frac{m_s m_b}{v^2} \approx 10^{-5}$. Equation (41) then gives large contribution to κ_s^H.

(ii) Equation (15) gives the typical magnitude of FCNC in class of models discussed in Sec. IIA. In case of Hermitian textures with $|F_{32}| = |F_{23}| \sim \frac{m_b}{v\cos\beta\sin\beta}|V_{L33}^* V_{L32}|$ we obtain $|F_{23}^* F_{32}| \sim 10^{-6}$ if $V_L \sim V$ leading to a sizable value of κ_s^H in this case also.

(iii) Models with $F_{32}^* = \frac{m_s}{m_b}F_{23}$ have additional suppression by $\frac{m_s}{m_b}$ compared to the previous estimates and one would need a light A to obtain significant κ_s^H. There is also an additional suppression by loop factors in MSSM but the F_{ij} can get enhanced by $\tan\beta$. Typical magnitude of F_{23} in MSSM is given by [19]

$$F_{23} \approx \frac{g|V_{tb}^* V_{ts}| m_b \epsilon_Y}{\sqrt{2}M_W}\tan^2\beta,$$

where ϵ_Y depends on the squark masses, the trilinear coupling A_t and μ. Taking the former two at TeV and $\mu \sim 300$ GeV, $\epsilon_Y \sim 0.002$ leading to $F_{23} \sim 2 10^{-6}\tan^2\beta$. Thus one can get significant effect only for very large $\tan\beta$.

The expression for B_H gets simplified in the decoupling limit corresponding to $M_A^2 \sim M_H^2 \gg M_Z^2, M_h^2$. In this limit, $\alpha - \beta \to \frac{\pi}{2}$ from Eq. (39) and the couplings $C_{S,S',P,P'}$ satisfy

$$\frac{C_S}{F_{23}} \approx \frac{C_S'}{F_{32}^*} \approx -\frac{C_P}{F_{23}} \approx \frac{C_P'}{F_{32}^*} \approx \frac{\sqrt{2}\pi m_\mu}{\alpha G_F V_{tb} V_{ts}^*}\frac{\sin\beta}{2v\cos\beta M_A^2}. \tag{42}$$

Because of this, the B_H in Eq. (34) reduces to

$$B_H = \frac{f_{B_s}^2 M_{B_s}^5 \tau_{Bs}}{128\pi(m_b + m_s)^2}\left(\frac{m_\mu^2}{v^2}\right)\frac{\tan^2\beta}{M_A^4}\left(1 - \frac{4m_\mu^2}{M_{B_s}^2}\right)^{1/2} \times \left(\left(1 - \frac{4m_\mu^2}{M_{B_s}^2}\right)|F_{23} - F_{32}^*|^2 + |F_{23} + F_{32}^*|^2\right). \quad (43)$$

The above equation allows us to derive simple correlation between κ_s^H and B_H. Combining Eqs. (40) and (43) we find

$$\begin{aligned} B_H &\approx \frac{4b\kappa_s^H \tan^2\beta}{\kappa M_A^2} \\ &\approx 2.2\times 10^{-8}\kappa_s^H\left(\frac{\tan\beta}{50}\right)^2\left(\frac{300\,\mathrm{GeV}}{M_A}\right)^2 \quad (\mathrm{Models}(A)\&(B)) \\ &\approx \frac{2b\kappa_s^H \tan^2\beta}{\kappa M_A^2}\frac{m_b}{m_s} \\ &\approx 1.7\times 10^{-8}\kappa_s^H\left(\frac{\tan\beta}{10}\right)^2\left(\frac{300\,\mathrm{GeV}}{M_A}\right)^2 \quad (\mathrm{Models}(C), \quad (44) \end{aligned}$$

where

$$b \equiv \frac{f_{B_s}^2 M_{B_s}^5 \tau_{B_s}}{128\pi(m_b + m_s)^2}\left(\frac{m_\mu}{v}\right)^2 \approx 1.1\times 10^4\ \mathrm{GeV}^4,$$

$$\kappa \equiv \frac{4\pi^2}{B_{B_s}\eta_B S_0(x_t) G_F^2 M_W^2 |V_{tb}^* V_{ts}|^2} \approx 2.2\times 10^{10}\ \mathrm{GeV}^2.$$

These correlations are independent of the magnitude and phases of the FCNC couplings and therefore test the assumption of (1) the presence of FCNC and (2) the MSSM structure in the Higgs potential independent of the detailed structures of the quark mass matrices. These correlations also show that the FCNC would lead to sizable B_H provided it gives significant correction to κ_s^H also.

Let us now turn to the numerical analysis. If we assume the MSSM-like Higgs structure then the allowed ranges of ϕ_{B_s} and C_{B_s} given in (38) determines the magnitude and phase of $F_{32}F_{23}^*$; see Eq. (40). The allowed region in $|\frac{F_{32}F_{23}^*}{M_A^2}|$-$\phi_s^H$ plane is shown in Fig. 1. No specific assumption is made on the nature of the FCNC couplings. Therefore Fig. 1 represents generic constraints on these couplings in all the 2HDM with tree level FCNC. The allowed values of $|F_{32}F_{23}^*|$ typically lie in the region $(1\text{–}5)\times 10^{-11} M_A^2\ \mathrm{GeV}^{-2}$ with a strong correlation between its magnitude and phase. A generic 2HDM need not follow the MSSM structure and the decoupling would also correspond to only a part of the available parameter space. We study departures from these assumptions numerically as follows. We randomly vary the Higgs masses M_h, M_H, M_A between the range 100–500 GeV keeping $M_h \le M_H$. The mixing angles α, β are varied in their full range. From every set of these input parameters we allow those which give C_{B_s}, ϕ_{B_s} in the range in Eq. (38) and the Br$(\bar{B}_s \to \mu^+\mu^-)$ below the limit in Eq. (2). In this random

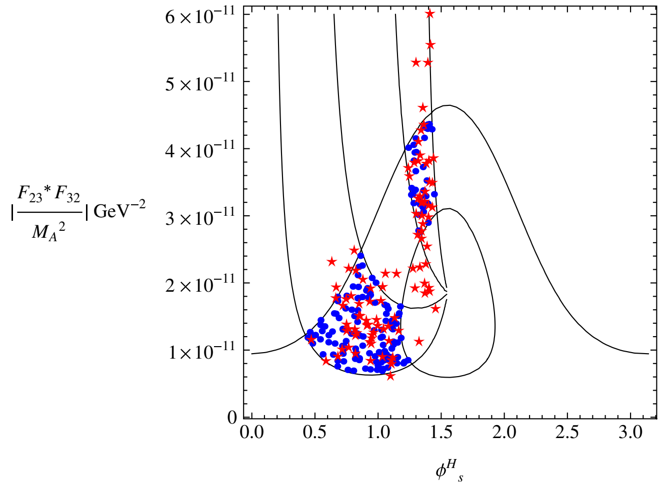

FIG. 1 (color online). The region in $|\frac{F_{32}F_{23}^*}{M_A^2}| - \phi_s^H$ allowed by the UTfit constraints on $B_s^0 - \bar{B}_s^0$ mixing. The solid lines and dots describe the region allowed under the assumption of the same Higgs potential as in MSSM. The stars correspond to assuming general Higgs sector and varying parameters as explained in the text.

analysis we distinguish two cases. One in which the MSSM relation Eq. (39) remains true. These cases are shown as dots in our figure while the more general case without that assumption is shown as $\star$.

Figure 2 shows the allowed region in the $\frac{|F_{32}|}{M_A}$-ϕ_s^H plane in classes of models which satisfy the constraints $F_{32} = \frac{m_s}{m_b}F_{23}^*$. One obtains the constraint $|F_{32}| \lesssim 1.2\times 10^{-6}\frac{M_A}{\mathrm{GeV}}$. This is to be compared with typical MSSM value $1.6\times 10^{-6}\tan^2\beta$. Thus one would need $\tan^2\beta \approx \frac{M_A}{\mathrm{GeV}}$ to account for the magnitude C_{B_s}. If F_{23} is given by Eq. (15) then

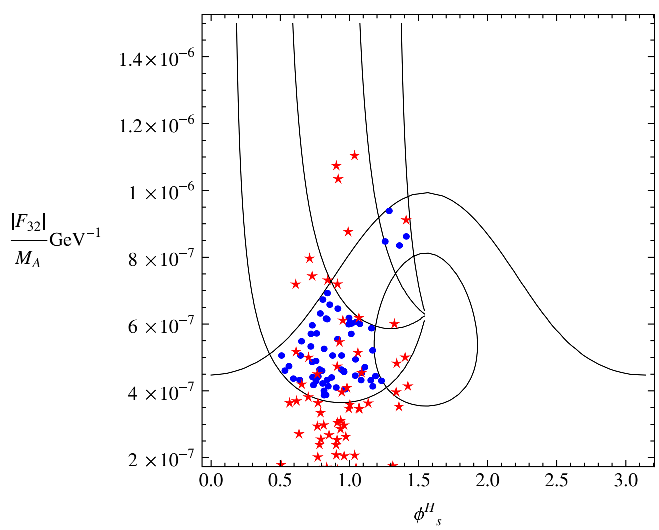

FIG. 2 (color online). The region in $|\frac{F_{32}}{M_A}| - \phi_s^H$ allowed by the $B_s^0 - \bar{B}_s^0$ mixing constraints in Eq. (38) in the class of models satisfying $F_{32} = \frac{m_s}{m_b}F_{23}^*$. Other details are as in Fig. 1.

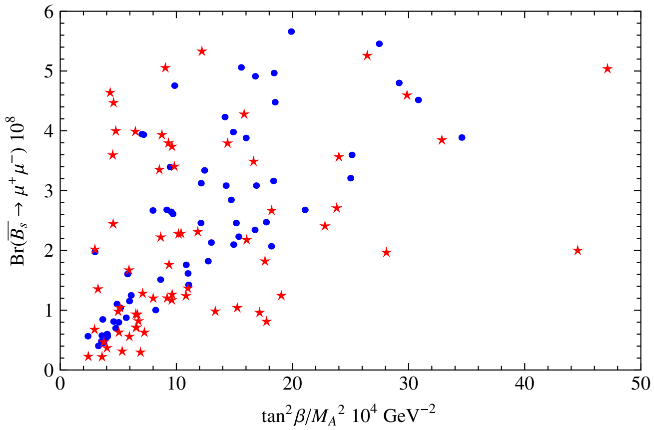

FIG. 3 (color online). Variations for the branching ratio of the process $\bar{B}_s \rightarrow \mu^+\mu^-$ with respect to $\tan^2\beta/M_A^2$ after incorporating the $B_s^0 - \bar{B}_s^0$ constraints in the model with $F_{32} = \frac{m_s}{m_b} F_{23}^*$. The dots and stars are defined as in Fig. 1.

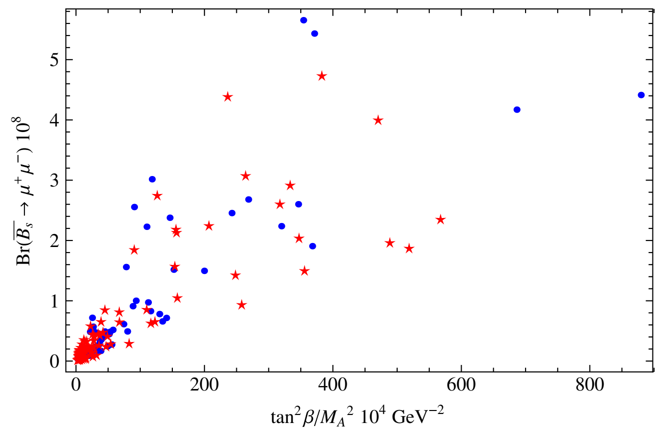

FIG. 5 (color online). Variations for the branching ratio of the process $\bar{B}_s \rightarrow \mu^+\mu^-$ with respect to $\tan^2\beta/M_A^2$ after incorporating the $B_s^0 - \bar{B}_s^0$ constraints in the model with $F_{32} = F_{23}^*$. The dots and stars are defined as in Fig. 1.

$F_{32} \approx 3 \times 10^{-5} \frac{1}{\sin\beta\cos\beta} \frac{.05}{|V_{L23}V_{L33}|}$. Thus, in this class of models one would need $|V_{L23}|$ somewhat smaller than $|V_{cb}| \sim 0.05$. In contrast to MSSM, large values of $\tan\beta$ are disfavored by the $B_s^0 - \bar{B}_s^0$ mixing constraint in this class of models.

Figure 3 shows the allowed values of the branching ratio for $\bar{B}_s \rightarrow \mu^+\mu^-$ obtained under the assumption $F_{32} = \frac{m_s}{m_b} F_{23}^*$ after imposing the UTfit constraints. It is possible to obtain relatively large branching ratios even for moderate values of $\tan\beta$ if M_A is light $\sim$100 GeV.

Figure 4 represents the corresponding constraints in class of models with Hermitian structure $F_{23} = F_{32}^*$. The required values for F_{32} are now (2–6) $\times 10^{-6} M_A$. But once again, one could obtain measurable rate for the dimuonic B_s decay even with moderate value of $\tan\beta$ as shown in Fig. 5.

Figure 6 displays the allowed values of $\bar{B}_s \rightarrow \mu^+\mu^-$ in the case $F_{23} = F_{32}$. It is seen that one needs relatively large $\tan\beta$ typically $\tan^2\beta/M_A^2 \approx 10^{-2}\ \mathrm{GeV}^{-2}$ in order to obtain a branching ratio larger than 10^{-8}. As already mentioned, this case also predicts vanishing Higgs-induced phase if the Higgs sector is CP conserving.

While $\bar{B}_s \rightarrow \mu^+\mu^-$ can receive significant contribution from the FCNC, the same is not the case with the semileptonic process $\bar{B}_d \rightarrow \bar{K}\mu^+\mu^-$. The FCNC induced contribution to this process can be qualitatively different than the 2HDM model based on the NFC. For example, if $F_{23} = F_{32}^*$ then Eqs. (34) and (35) together imply that only the scalar Higgses contribute to $\bar{B}_d \rightarrow \bar{K}\mu^+\mu^-$ while $\bar{B}_s \rightarrow \mu^+\mu^-$ gets contribution from the pseudoscalar Higgs. Thus these processes are uncorrelated if the corresponding

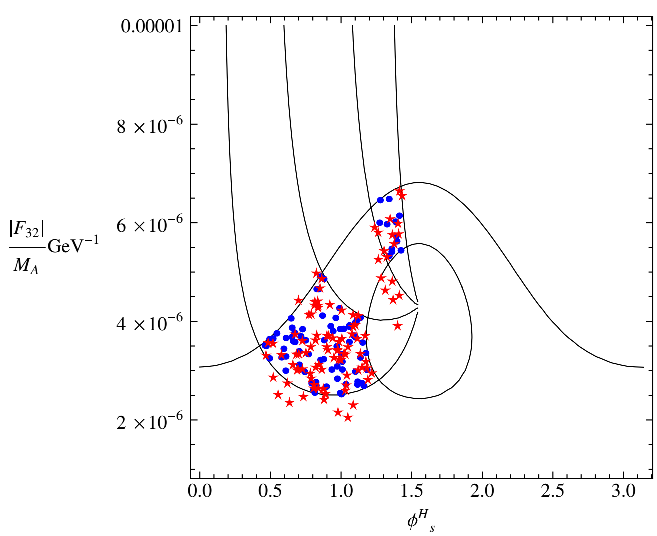

FIG. 4 (color online). The region in $|\frac{F_{32}}{M_A}| - \phi_s^H$ allowed by the $B_s^0 - \bar{B}_s^0$ mixing constraints in Eq. (38) in the class of models satisfying $F_{32} = F_{23}^*$. Other details are as in Fig. 1.

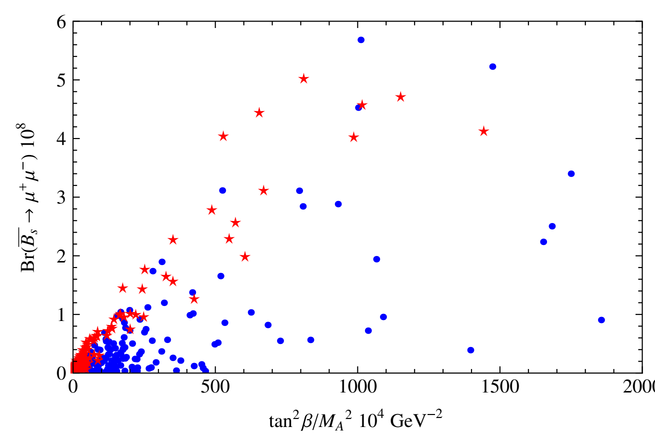

FIG. 6 (color online). Variations for the branching ratio of the process $\bar{B}_s \rightarrow \mu^+\mu^-$ with respect to $\tan^2\beta/M_A^2$ after incorporating the $B_s^0 - \bar{B}_s^0$ constraints in the model with $F_{32} = F_{23}$. The dots and stars are defined as in Fig. 1.

Higgs masses are not correlated. This is to be compared with the standard 2HDM or the MSSM where definite correlations between these processes have been pointed out [40]. At the quantitative level, we find numerically that after imposition of the $B_s^0 - \bar{B}_s^0$ mixing, the allowed numerical values of the couplings $\tilde{C}_{S,P}$ in all cases are such that the Higgs contribution to the branching ratio of $\bar{B}_d \to \bar{K}\mu^+\mu^-$ amounts to at most few percent of the SM contribution. This is much smaller than the theoretical uncertainties. Therefore detecting Higgs effects in this branching ratio would need considerable reduction in theoretical errors. However one can conclude that if a significant new physics contribution to the branching ratio of this process is detected, it cannot be due to the presence of the Higgs-induced FCNC.

V. CONCLUSION

$b \to s$ transition is known to be a good probe of physics beyond the standard model. We have looked at the possibility of using this transition to test the Higgs-induced FCNC assuming that the neutral Higgs provides the dominant contribution. In this case, several processes get described in terms of two complex parameters, F_{23} and F_{32}, and the Higgs mass parameters through Eq. (8). Phenomenological analysis in many of the earlier works [29] used the specific form for F_{23} and F_{32} motivated by the Cheng-Sher ansatz and often considered them to be real. We have tried to develop model-independent constraints on these parameters. In particular, as shown here, the phases of the FCNC couplings can play an important role and may provide the large CP violating phase that may be needed to explain the CDF and D0 results on CP violation. We discussed phenomenology of three broad classes of theories with FCNC satisfying the relations (1) $F_{23} = F_{32}^*$, (2) $F_{23} = F_{32}$, and (3) $F_{32} = \frac{m_s}{m_b} F_{23}^*$. We discussed several textures of the Yukawa couplings giving rise to these relations. In particular, MSSM and 2HDM with NFC provide examples of (3). We showed that the case (2) cannot account for large CP violating phase if the Higgs sector is CP conserving. The same applies to MSSM and the particularly predictive model of [27]. Our numerical analysis shows that one typically needs $F_{32} \sim (10^{-6} - 10^{-7}) M_A\ \mathrm{GeV}^{-1}$. As discussed here such values can arise within the textures discussed in Sec. II.

Using the available information on the $B_s^0 - \bar{B}_s^0$ mixing we have worked out expectations for the leptonic branching ratio $\bar{B}_s \to \mu^+\mu^-$. It is found that the former constraints do allow measurable values for this branching ratio but the range for $\frac{\tan^2\beta}{M_A^2}$ required in these cases are different as seen from Figs. 3, 5, and 6. In contrast, the Higgs contribution to the branching ratio of process $\bar{B}_d \to \bar{K}\mu^+\mu^-$ is constrained to be close to or smaller than the SM value in all these models. Thus any significant deviation in this branching ratio compared to the SM prediction will rule out all the models with FCNC in one shot under the assumption that these models are the only source of new physics in the $B_s^0 - \bar{B}_s^0$ mixing.

ACKNOWLEDGMENTS

We thank Namit Mahajan for several useful discussions.

[1] A. Lenz and U. Nierste, J. High Energy Phys. 06 (2007) 072; B. Dutta and Y. Mimura, Phys. Rev. D **75**, 015006 (2007); U. Nierste, Nucl. Phys. B, Proc. Suppl. **170**, 135 (2007); P. Ball, arXiv:hep-ph/0612325; F. J. Botella, G. C. Branco, and M. Nebot, Nucl. Phys. **B768**, 1 (2007); A. Datta and P. J. O'Donnell, Phys. Rev. D **72**, 113002 (2005); A. Datta, Phys. Rev. D **74**, 014022 (2006).

[2] P. Ball and R. Fleischer, Eur. Phys. J. C **48**, 413 (2006); P. Ball, arXiv:hep-ph/0703214; E. Lunghi and A. Soni, J. High Energy Phys. 08 (2009) 051.

[3] A. J. Buras and D. Guadagnoli, Phys. Rev. D **78**, 033005 (2008).

[4] M. Bona *et al.* (UTfit Collaboration), arXiv:0803.0659; http://www.utfit.org.

[5] O. Deschamps, arXiv:0810.3139; J. Charles *et al.*, http://ckmfitter.in2p3.fr.

[6] A. J. Lenz, arXiv:0808.1944; Nucl. Phys. B, Proc. Suppl. **177–178**, 81 (2008).

[7] V. M. Abazov *et al.* (D0 Collaboration), Phys. Rev. Lett. **101**, 241801 (2008).

[8] T. Aaltonen *et al.* (CDF Collaboration), Phys. Rev. Lett. **100**, 161802 (2008).

[9] Heavy Flavor Averaging Group (HFAG), http://www.slac.stanford.edu/xorg/hfag/osc/PDG_2009/#BETAS.

[10] M. Bona *et al.*, arXiv:0906.0953.

[11] M. Blanke, A. J. Buras, D. Guadagnoli, and C. Tarantino, J. High Energy Phys. 10 (2006) 003.

[12] T. Aaltonen *et al.* (CDF Collaboration), Phys. Rev. Lett. **100**, 101802 (2008).

[13] C. Bobeth, T. Ewerth, F. Kruger, and J. Urban, Phys. Rev. D **64**, 074014 (2001).

[14] C. Bobeth, G. Hiller, and G. Piranishvili, J. High Energy Phys. 12 (2007) 040.

[15] See, for example, G. Isidori, arXiv:0801.3039.

[16] S. Jager, Eur. Phys. J. C **59**, 497 (2009).

[17] K. S. Babu and C. F. Kolda, Phys. Rev. Lett. **84**, 228 (2000).

[18] C. S. Huang, W. Liao, and Q. S. Yan, Phys. Rev. D **59**, 011701 (1998).

[19] A. J. Buras, P. H. Chankowski, J. Rosiek, and L. Slawianowska, Nucl. Phys. **B659**, 3 (2003).

[20] J. F. Gunion, H. E. Haber, G. L. Kane, and S. Dawson, *The Higgs Hunter's Guide* (Addison-Wesley, Reading, MA, 1990).

[21] S. L. Glashow and S. Weinberg, Phys. Rev. D **15**, 1958 (1977).

[22] G. D'Ambrosio, G. F. Giudice, G. Isidori, and A. Strumia, Nucl. Phys. **B645**, 155 (2002).

[23] B. Dutta and Y. Mimura, Phys. Lett. B **677**, 164 (2009); K. Kawashima, J. Kubo, and A. Lenz, Phys. Lett. B **681**, 60 (2009).

[24] A. Antaramian, L. J. Hall, and A. Rasin, Phys. Rev. Lett. **69**, 1871 (1992); L. J. Hall and S. Weinberg, Phys. Rev. D **48**, R979 (1993).

[25] T. P. Cheng and M. Sher, Phys. Rev. D **35**, 3484 (1987).

[26] A. S. Joshipura, Mod. Phys. Lett. A **6**, 1693 (1991).

[27] G. C. Branco, W. Grimus, and L. Lavoura, Phys. Lett. B **380**, 119 (1996).

[28] D. Atwood, L. Reina, and A. Soni, Phys. Rev. Lett. **75**, 3800 (1995); Phys. Rev. D **53**, 1199 (1996); **55**, 3156 (1997); E. Lunghi and A. Soni, J. High Energy Phys. 09 (2007) 053.

[29] Y. L. Wu and Y. F. Zhou, Phys. Rev. D **61**, 096001 (2000); C. S. Huang and J. T. Li, Int. J. Mod. Phys. A **20**, 161 (2005); Z. j. Xiao and L. Guo, Phys. Rev. D **69**, 014002 (2004).

[30] G. Isidori and A. Retico, J. High Energy Phys. 11 (2001) 001; H. E. Logan and U. Nierste, Nucl. Phys. **B586**, 39 (2000), and reference therein.

[31] R. G. Roberts, A. Romanino, G. G. Ross, and L. Velasco-Sevilla, Nucl. Phys. **B615**, 358 (2001).

[32] G. Ross and M. Serna, Phys. Lett. B **664**, 97 (2008).

[33] I. Dorsner and A. Y. Smirnov, Nucl. Phys. **B698**, 386 (2004).

[34] A. S. Joshipura and B. P. Kodrani, Phys. Rev. D **77**, 096003 (2008).

[35] A. E. Carcamo, R. Martinez, and J. A. Rodriguez, Eur. Phys. J. C **50**, 935 (2007).

[36] A. S. Joshipura and B. P. Kodrani, Phys. Lett. B **670**, 369 (2009).

[37] A. J. Buras, arXiv:hep-ph/0101336.

[38] G. Buchalla, A. J. Buras, and M. E. Lautenbacher, Rev. Mod. Phys. **68**, 1125 (1996).

[39] M. Wirbel, B. Stech, and M. Bauer, Z. Phys. C **29**, 637 (1985); A. Ali, P. Ball, L. T. Handoko, and G. Hiller, Phys. Rev. D **61**, 074024 (2000).

[40] A. K. Alok, A. Dighe, and S. Uma Sankar, arXiv:0803.3511; Phys. Rev. D **78**, 034020 (2008); **78**, 114025 (2008).